



Differentiating peritoneal tuberculosis and peritoneal carcinomatosis based on a machine learning model with CT: a multicentre study

Yu Pang^{1,2} · Ye Li³ · Dong Xu³ · Xiaoli Sun⁴ · Dailun Hou³

Received: 22 April 2022 / Revised: 14 November 2022 / Accepted: 14 November 2022 / Published online: 13 March 2023
© The Author(s), under exclusive licence to Springer Science+Business Media, LLC, part of Springer Nature 2023

Abstract

Purpose It is still a challenge to make early differentiation of peritoneal tuberculosis (PTB) and peritoneal carcinomatosis (PC) clinically as well as on imaging and laboratory tests. We aimed to develop a model to differentiate PTB from PC based on clinical characteristics and primary CT signs.

Methods This retrospective study included 88 PTB patients and 90 PC patients (training cohort: 68 PTB patients and 69 PC patients from Beijing Chest Hospital; testing cohort: 20 PTB patients and 21 PC patients from Beijing Shijitan Hospital). The images were analyzed for omental thickening, peritoneal thickening and enhancement, small bowel mesentery thickening, the volume and density of ascites, and enlarged lymph nodes (LN). Meaningful clinical characteristics and primary CT signs comprised the model. ROC curve was used to validate the capability of the model in the training and testing cohorts.

Results There were significant differences in the following aspects between the two groups: (1) age; (2) fever; (3) night sweat; (4) cake-like thickening of the omentum and omental rim (OR) sign; (5) irregular thickening of the peritoneum, peritoneal nodules, and scalloping sign; (6) large ascites; and (7) calcified and ring enhancement of LN. The AUC and F1 score of the model were 0.971 and 0.923 in the training cohort and 0.914 and 0.867 in the testing cohort.

Conclusion The model has the potential to distinguish PTB from PC and thus has the potential to be a diagnostic tool.

Keywords Peritoneal tuberculosis · Peritoneal carcinomatosis · Computed tomography · Machine learning

Introduction

Tuberculosis (TB) is a communicable disease and one of the leading causes of death globally [1]. Before the coronavirus (COVID-19) pandemic, TB has been the top cause of death from a single infectious agent [1]. *Mycobacterium Tuberculosis*

(MTB) can involve any part of body such as the meninges, the abdomen or the retina via blood or lymphatic [2]. Peritoneal TB (PTB) is one of the commonest manifestations of abdominal TB [3]. The diagnosis of this disease still poses a great challenge and may be delayed due to the nonspecific clinical presentation, radiologic, histologic, and molecular techniques [4].

Peritoneal carcinoma (PC) is a malignant tumor of the peritoneum, which can be primary or secondary, infiltrating into the peritoneum and proliferating on its surface [5]. It can be challenging to differentiate PTB from PC either on clinical or imaging [6]. Computed tomography (CT) has shown good performance as a diagnostic tool, monitoring imaging changes and screening method for detecting peritoneal lesions. Several studies have compared PTB with PC on CT [7, 8]. However there have been different viewpoints in meaningful CT findings and significant overlaps between the two persists [7, 8]. Some clinical studies recommended laparoscopy as the most important tool to differentiate PTB from PC [9, 10]. However, laparoscopic biopsies are invasive as well as expensive. As a result, it is necessary to develop an accurate and non-invasive method of PTB identification.

Yu Pang and Ye Li have contributed equally to this work.

✉ Xiaoli Sun
sunxiaoli2886@bjsjth.cn

✉ Dailun Hou
houdailun@163.com

¹ School of Management, Hefei University of Technology, Hefei, China

² Department of Artificial Intelligence, Beijing Chest Hospital, Capital Medical University, Beijing, China

³ Department of Radiology, Beijing Chest Hospital, Capital Medical University, Beijing 101149, China

⁴ Department of Radiology, Beijing Shijitan Hospital, Capital Medical University, Beijing 101149, China

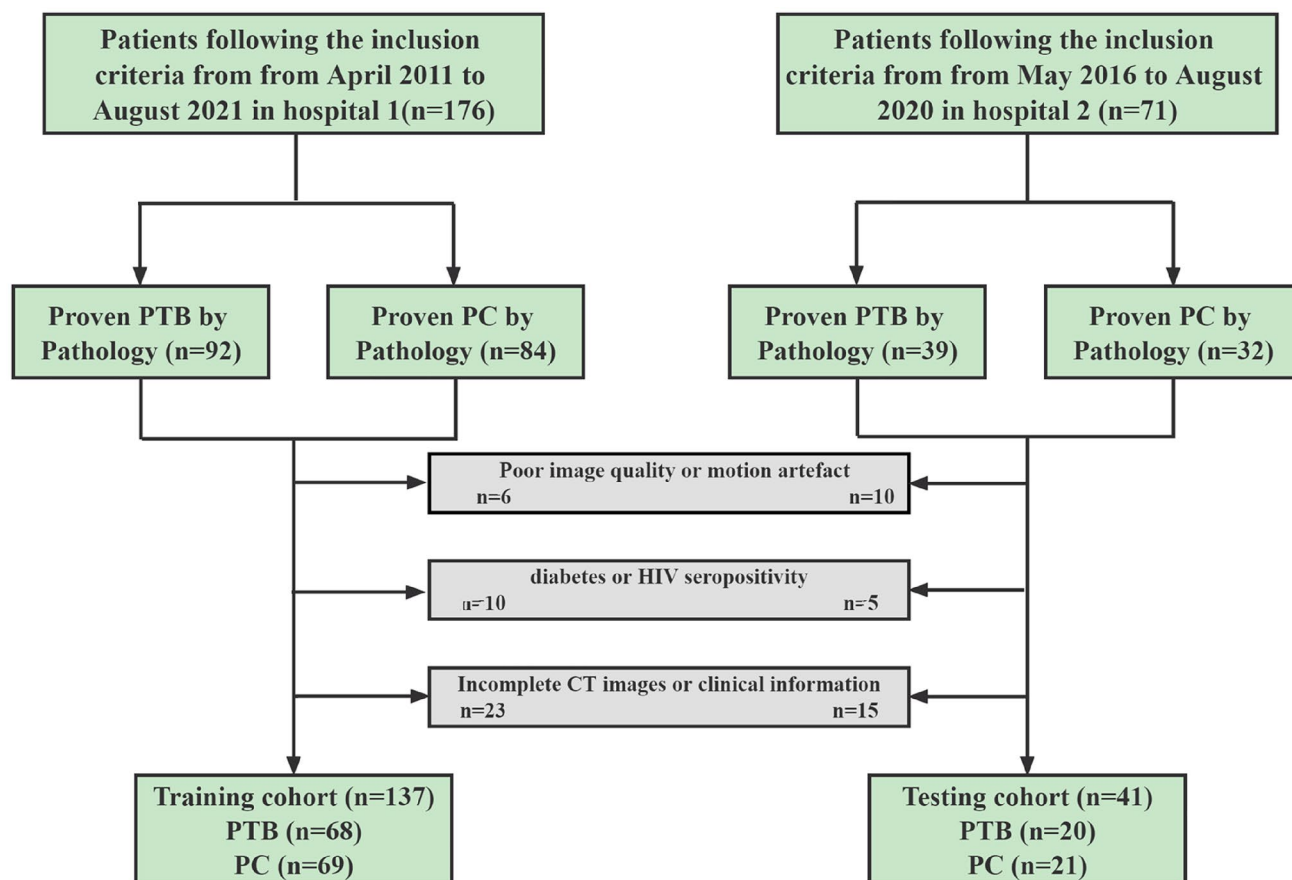


Fig. 1 The flowchart of patient selection

We hypothesized that the CT findings of PTB and PC may be useful for discriminating these two diseases. The aim of this study was to evaluate whether CT findings could distinguish PTB from PC and develop a simple discrimination model successfully.

Materials and methods

Participants

This retrospective study was approved by the ethics of the local hospital and the requirement for informed consent was waived.

In the study, all patients were enrolled according to the inclusion and exclusion criteria. The inclusion criteria were as follows: (a) the diagnosis of PTB was the combination of positive cultures for MTB, demonstration of caseating granulomata on pathology and clinical improvement after anti-tuberculosis treatment; PC was confirmed by pathology or demonstration of malignant cells in the ascitic fluid;

(b) all patients underwent enhanced abdominal CT with informed consent; (c) all CT scans were performed before biopsy, chemotherapy, radiotherapy, or surgery. The exclusion criteria included the following: (a) poor image quality or motion artefact; (b) diabetes or HIV seropositivity; (c) incomplete CT images or clinical information.

According to the criteria, as shown in Fig. 1, we recruited a total of 88 patients with PTB and 90 patients with PC. Specifically, 68 patients with PTB and 69 patients with PC from hospital 1 were enrolled as the training cohort from April 2011 to August 2021. In addition, a testing cohort from hospital 2 was subsequently enrolled, including 20 patients with PTB and 21 patients with PC from May 2016 to August 2020.

CT image acquisition

All CT examinations were performed by Revolution CT (GE Healthcare, USA), or Brilliance CT (Philips Healthcare, the Netherlands). The scanning parameters were as follows: tube current, 100–250 mAs; tube voltage, 100–120 kV;

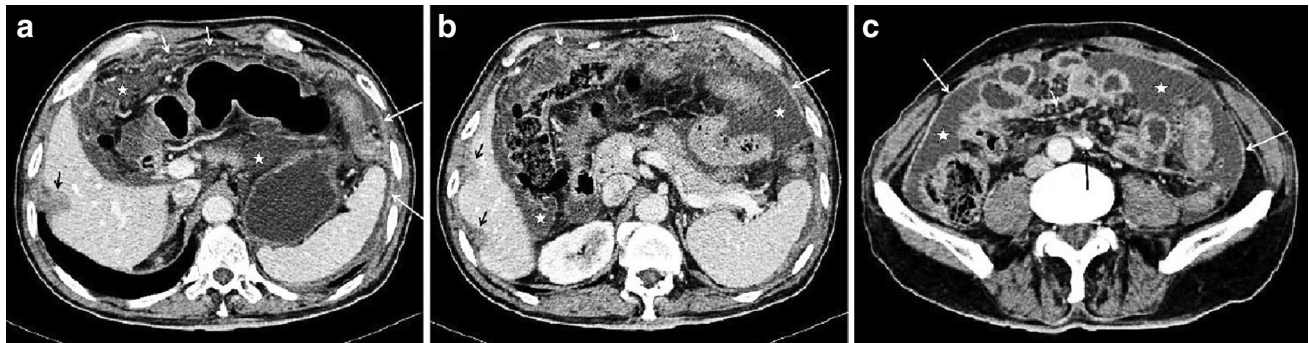


Fig. 2 Axial CT section through the abdomen in the venous phase in a 67-year-old man with PTB. **a, b, c** Smooth thickening of the peritoneum (long white arrow), smudged thickening of the omentum (short

white arrow), scalloping sign (short black arrow), high-density ascites (star) and calcified LN (long black arrow)

collimation, 1 mm; pitch, 1; reconstruction interval, 0.5 mm; and acquisition matrix, 512×512 . All patients underwent contrast-enhanced CT scanning simultaneously using multi-phase scan protocols. Precontrast, arterial phase (30–40 s), portal vein phase (70–90 s), and delay phase (120–180 s) were obtained. 80 mL of nonionic contrast material (Iopamidol, 300 mgI/mL) was injected intravenously at a flow rate of 2.5–3.0 mL/s.

Image analysis

All images were analysed on Extended Brilliance Workspace (EBW). Original transverse and post-processed images which included maximum intensity projection (MIP) and multiple-planar reconstruction (MPR) images were reviewed for each patient. CT images were independently reviewed by two radiologists with at least 10 years of experience in analysing abdominal images who were

blinded to the final clinical diagnosis. The primary signs were as follows:

(a) Omental thickening was classified as smudged (infiltration with unclear soft tissue density) (Fig. 2), nodular (Fig. 3), cake-like (soft-tissue replacement) (Fig. 4) in those with diffuse enhancement and the omental rim (OR) sign [7] which defined as the whole or part of the omentum was clearly observed in the venous phase, regardless of omental thickness (thin or thick) and enhancement (moderate or significant) (Fig. 5).

(b) Peritoneal involvement included diffuse smooth thickening (Fig. 2), irregular thickening focally, peritoneal nodules (Fig. 6), whether peritoneal enhanced and scalloping sign (Fig. 2). The scalloping sign [11] was defined as the indentations of the visceral surfaces of intraperitoneal organs.

(c) Small bowel mesentery thickening was defined as diffuse increased density with soft-tissue density masses



Fig. 3 Axial CT section through the abdomen in the venous phase in a 66-year-old man with PC. Scalloping sign (long white arrow), nodular thickening of the omentum (short white arrow) and high-density ascites (star)



Fig. 4 Axial CT section through the abdomen in the venous phase in a 56-year-old woman with PC. Cake-like thickening of the omentum (long white arrow), diffuse thickening of the mesentery (short white arrow) and high-density ascites (star)

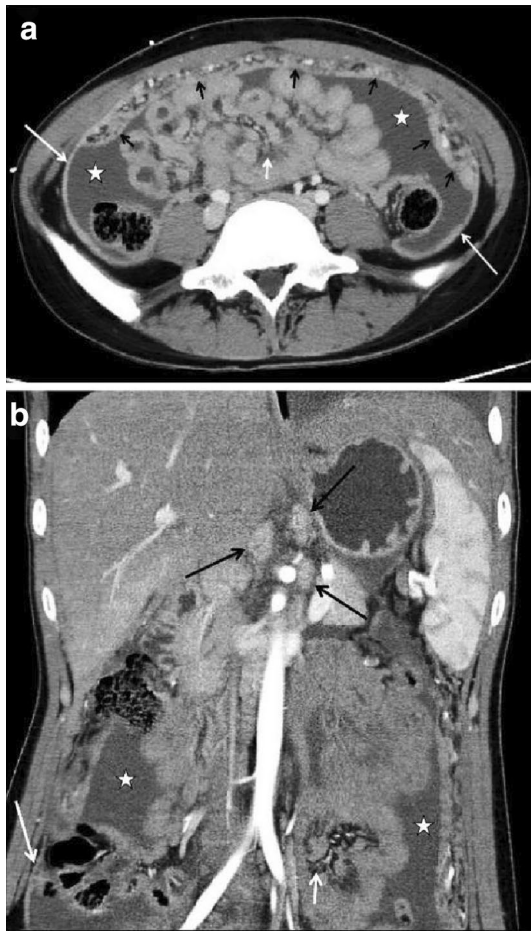


Fig. 5 Axial and coronal CT section through the abdomen in the venous phase in a 20-year-old woman with PTB. **a, b** Smooth thickening of the peritoneum (long white arrow), thickened with crowded vascular bundles of the mesentery (short white arrow), OR sign (short black arrow) and high-density ascites (star)

(Fig. 4), thickened with crowded vascular bundles (Fig. 5) and mesenteric nodules.

(d) The volume and density of ascites were documented. Ascites were considered hyperdense when more than 20 HU (Fig. 2) and hypo when less. The volume of ascites was classified as large, moderate and slight ascites. It was considered large when it filled the entire abdomen and pressed the organs and peritoneum, moderate when it localized around the liver, spleen or bilateral paracolic sulcus and small when it located predominantly in the pelvis.

(e) The enlargement and enhancement of lymph nodes (LN) were also documented. The enlarged LN was defined as the short axis diameter was more than 1 cm in the retroperitoneal and mesenteric stations (Fig. 6). In addition, the presence of calcification (Fig. 2), necrosis and ring enhancement of LN were also looked for.

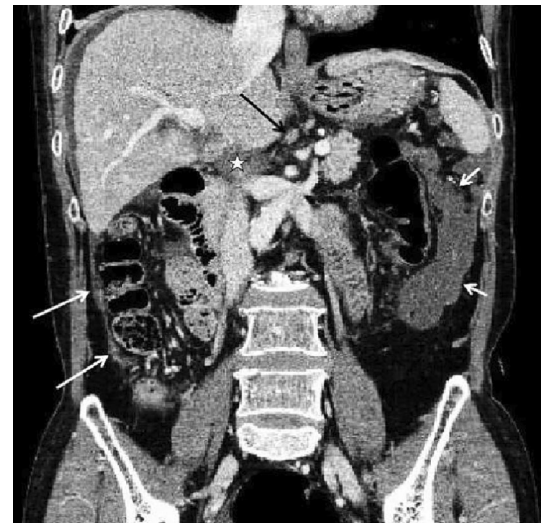


Fig. 6 Coronal CT section through the abdomen in the venous phase in a 50-year-old woman with PC. Peritoneal nodules of the peritoneum (long white arrow), cake-like thickening of the omentum (short white arrow), enlarged LN (long black arrow) and high-density ascites (star)

Statistical analysis and model construction

Statistical analysis was performed with SPSS software (version 21) and the Python Scikit-learn package. Kappa test was used to evaluate the two radiologists agreements of primary CT signs (κ values of poor, fair, moderate, substantial, and near-perfect agreement were < 0.00 , $0.21-0.40$, $0.41-0.60$, $0.61-0.80$, and $0.81-1.00$, respectively). For the qualitative analysis, the Pearson chi-square test was used for categorical variables. For quantitative analysis, Student's *t* test was used for normally distributed continuous variables. Statistical tests were conducted with $p < 0.05$ as an indicator of statistical significance.

In the training cohort, both the clinical characteristics and primary CT signs with significant differences were selected to build a model by logistic regression. It was a traditional machine learning model in medical applications and recently used in the field. The model was trained and validated on the training cohort which were randomly divided into two parts by the ratio of 7:3 using five-fold cross validation. Finally, the best model which was separately selected was tested on the external testing cohort.

The performance of the model in both cohorts was evaluated with receiver operator characteristic (ROC) curve, and the area under the curve (AUC) was calculated. In addition, the accuracy, precision (positive predictive value), recall (sensitivity) and F1 score in both two cohorts. F1 score is the harmonic average of the precision and recall, ranging from 0 to 1.

Table 1 Clinical characteristics from PTB and PC in training cohort and testing cohort

Clinical characteristics	Training cohort		<i>p</i> -value	Testing cohort		<i>p</i> -value
	PTB(<i>n</i> =68)	PC(<i>n</i> =69)		PTB(<i>n</i> =20)	PC(<i>n</i> =21)	
Gender, <i>n</i> (%)						
Male	37(54.41)	32(46.38)	0.347	13(65.00)	9(42.86)	0.155
Female	31(45.59)	37(53.62)		7(35.00)	12(57.14)	
Age (mean ± SD years)	48.48 ± 19.64	56.22 ± 10.69	0.020*	47.55 ± 19.13	57.52 ± 10.28	0.043*
Fever, <i>n</i> (%)	26(38.24)	2(2.90)	0.00*	7	0	0.003*
Abdominal pain, <i>n</i> (%)	34(50.00)	26(37.68)	0.146	11	8	0.278
Abdominal distention, <i>n</i> (%)	41(60.29)	37(53.62)	0.430	14	12	0.393
Night sweat, <i>n</i> (%)	20(29.41)	0(0.00)	0.00*	5	0	0.014*

Differences were assessed by Student's *t* test or chi-square test. *SD* standard deviation. **p* < 0.05

Results

Patient clinical characteristics

The clinical characteristics of all 178 patients were listed in Table 1. As shown in Table 1, there were significant differences in age, fever and night sweat between PTB patients and PC patients in both the training and testing cohorts (*p* < 0.05). Besides, the gender, abdominal pain, and distention of PTB and PC patients had no significant difference in either the training cohort or testing cohort.

Primary CT signs (Table 2)

There was excellent interobserver agreement with regard to the primary signs of omentum, peritoneum, mesentery, ascites, LN and scalloping sign (*k* = 0.772, 0.783, 0.887, 0.837, 0.894, and 0.864, respectively).

Omentum

Most PTB and PC patients showed omental thickening and there was no significant differences between two groups. Specifically, cake-like thickening of the omentum was more frequently observed in PC patients than PTB patients in both two cohorts (*p* < 0.05). Besides, there was significant difference in OR sign between two groups (*p* < 0.05). The remaining signs (smudged thickening and nodular thickening) had no significant difference in two groups.

Peritoneum

The irregular thickening and nodules of peritoneum were more frequent in PC patients than PTB patients between two cohorts (*p* < 0.05). As for the smooth thickening of peritoneum and peritoneal enhancement, there were no significant difference in

two groups. There was significant difference with the scalloping sign between PTB patients and PC patients in two cohorts (*p* < 0.05).

Mesentery

The primary signs of mesentery including diffuse thickening, thickened with crowded vascular bundles, and mesenteric nodules showed no significant difference between PTB and PC patients in either training cohort or testing cohort.

Ascites

Large ascites was more common in PC patients than PTB patients in both two cohorts (*p* < 0.05). Besides, slight ascites, moderate ascites and the density of ascites showed no significant difference between two groups.

LN

Among the signs of LN, there were significant differences in calcified LN and the ring enhancement of LN between two groups (*p* < 0.05). The remaining signs including enlarged LN and LN with necrosis had no significant differences in two cohorts.

Model performance

As a result, 11 variables were selected to build the model which included three significant clinical characteristics and eight primary CT signs. The ROC curves and AUCs of the model in the training and testing cohorts are shown in Fig. 7. The model showed a favorable discriminatory ability in the training cohort, with an AUC of 0.971 and F1 score of 0.923, which was confirmed in the testing cohort AUC of 0.914 and F1 score of 0.867. In addition, the accuracy, precision and recall of the model in both the training cohort were 0.927,

Table 2 Primary CT signs from PTB and PC in training cohort and testing cohort

CT signs	Training cohort		<i>p</i> -value	Testing cohort		<i>p</i> -value
	PTB	PC		PTB	PC	
	(<i>n</i> = 68)	(<i>n</i> = 69)		(<i>n</i> = 20)	(<i>n</i> = 21)	
Omentum, <i>n</i> (%)						
Smudged thickening	27(39.71)	23(33.33)	0.439	9	7	0.444
Nodular thickening	11(16.18)	16(23.19)	0.302	4	6	0.523
Cake-like thickening	9(13.24)	26(37.68)	0.001*	2	8	0.036*
OR sign	12(17.65)	2(2.90)	0.004*	4	0	0.031*
Peritoneum, <i>n</i> (%)						
Smooth thickening	12(17.65)	5(7.25)	0.065	6	3	0.224
Irregular thickening	0(0)	15(21.74)	0.000*	0	4	0.040*
Peritoneal nodules	31(45.59)	47(68.12)	0.008*	5	12	0.037*
Peritoneal enhancement	22(32.35)	18(26.09)	0.420	7	8	0.837
Scalloping sign	2(2.94)	37(53.62)	0.000*	0	9	0.001*
Mesentery, <i>n</i> (%)						
Diffuse thickening	5(7.35)	7(10.14)	0.563	1	2	0.578
Thickened with crowded vascular bundles	39(57.35)	43(62.32)	0.553	11	13	0.654
Mesenteric nodules	7(10.29)	6(8.70)	0.750	2	3	0.675
Ascites, <i>n</i> (%)						
High-density ascites	32(47.06)	23(33.33)	0.101	10	9	0.647
Low-density ascites	29(42.65)	40(57.97)	0.073	8	11	0.427
Slight ascites	19(27.94)	16(23.19)	0.524	6	6	0.920
Moderate ascites	16(23.53)	8(11.59)	0.066	5	4	0.645
Large ascites	26(38.24)	39(56.52)	0.032*	7	14	0.043*
LN, <i>n</i> (%)						
Enlarged LN	26(38.24)	18(26.09)	0.128	8	7	0.658
Calcified LN	12(17.65)	2(2.90)	0.004*	4	0	0.031*
LN with necrosis	10(14.71)	4(5.80)	0.085	4	1	0.136
Ring enhancement of LN	12(17.65)	1(1.45)	0.001*	5	0	0.014*

Differences were assessed by chi-square test. **p* < 0.05

1.00, and 0.857, which was confirmed in the testing cohort 0.857, 1.00, and 0.765.

Discussion

In order to prevent morbidity, it is essential to make early diagnosis of diffuse peritoneal disease and differentiation between PTB and PC. However, it is still a challenge to make early identification clinically as well as on imaging and laboratory tests. The main finding of this study is that we developed a machine learning model for differentiating PTB from PC based on significant clinical characteristics and primary CT signs, which achieved good accuracy in an independent external testing cohort.

The analysis of clinical characteristics showed that the age of PTB patients had significant difference with PC patients, whereas sex did not show significant difference, similar to the results of previous studies [12]. Most patients

with PTB are young or middle-aged [4] and patients with PC are old-aged [13]. PTB is a chronic inflammation caused by infection with MTB [2]. Besides, fever and night sweat were the typical symptoms as reported in previous studies [14, 15]. Our results are consistent with other studies [8]. It was hardly seen that PC patients had fever and night sweat. There were significant differences in fever and night sweat between two groups. These clinical findings may be helpful for differentiating PTB from PC. As for abdominal distention and pain, they were the most common initial symptoms of the two diseases [8]. These atypical and nonspecific symptoms had no significant difference between two groups.

The omentum of most patients in our study was thickened and similar to previous studies [16, 17]. Our study found that the cake-like thickening of the omentum was more frequent in PC patients than PTB patients (*p* < 0.05) as well as several studies [7, 8]. This sign was predominant in PC and a good sign to rule out PTB. It is reported to be frequently associated with higher grade, non-mucinous and invasive tumors

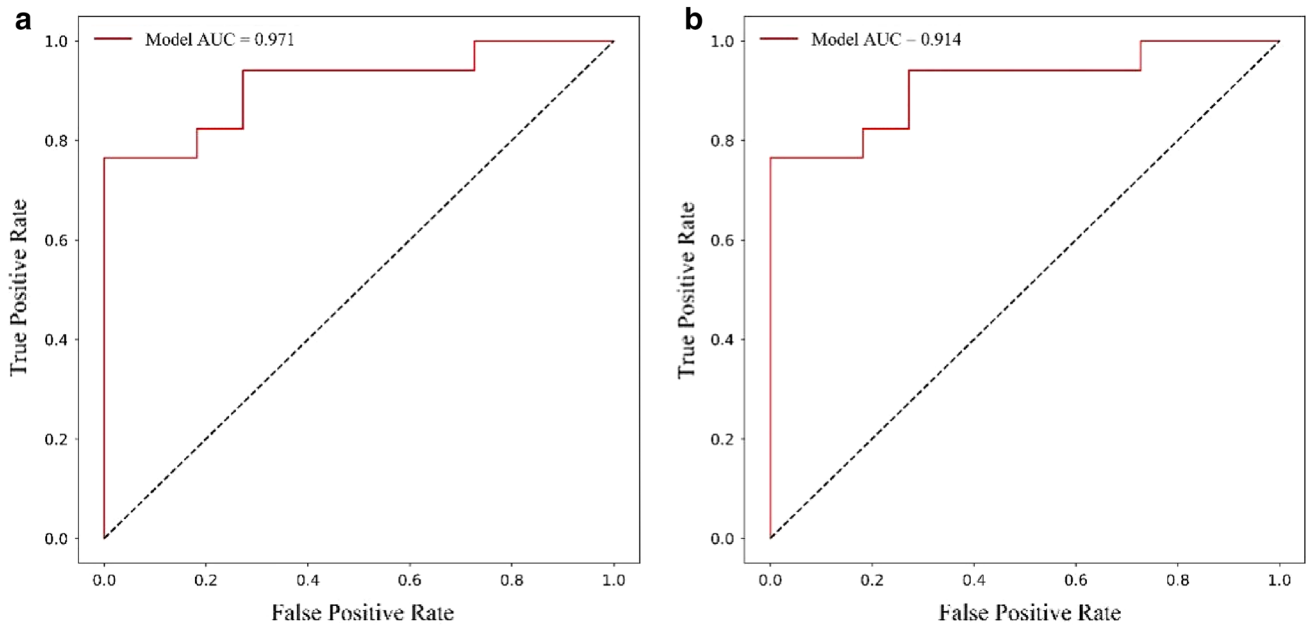


Fig. 7 ROC curves of the model. **a** Training cohort **b** Testing cohort

[18]. The smudged and nodular type were the common form of omentum with PTB [19]. However, there were no significant difference between two groups. The omental changes in PC were associated with irregular tumor growth, while changes in PTB were associated with inflammatory hyperemia and edema. Ramanan et al., mentioned the OR sign, which is circular in morphology outlining the perimeter of the omentum whether thick or thin [7]. Actually, we found the OR sign to be highly specific of PTB as well as previous study. However, the frequency of OR sign in our study was lower than previous reported. PTB triggers a fairly diffuse and uniform inflammation. Hence, the fat density substance of the omentum provides a high contrast clearly outlining this peritoneal enhancement as a rim around it.

Peritoneal changes were thought to be the strongest differentiator of PTB from PC [20] and a previous study suggested that smooth thickening of the peritoneum was the most specific predictor of PTB [6]. However, there was no significant difference in our study. Irregular thickening of the peritoneum and peritoneal nodules had significant differences between two groups. These differences may be caused by CT section thickness. The thinner section which increased resolution and picked up more of the subtle focal characteristics. The enhancement of the peritoneum did not differentiate PTB from PC, which was similar to previous study [21]. It is reported that scalloping sign may suggest PC [22]. In our study too, the scalloping sign was more frequent in PC than PTB. This sign may be caused mainly by large peritoneal deposits.

The most common type of mesenteric thickening was thickened with crowded vascular bundles in both two groups [23]. Specifically, it includes a stellate pattern which is due to perivascular bundle thickening that causes the normal fat to highlight mesenteric vessels or pleated appearance of the mesentery with fixation of bowel loops which shows soft-tissue thickening of the mesentery leaves [24]. The thickening mesentery result from tumorous soft tissue of PC and edema of PTB. This sign had no significant difference in two groups.

Most patients in our study had ascites between two groups. The density of ascites had no significant difference in two groups. Ascites may be clear in early stage and have a high density in late stage when it is filled with high protein and cellular contents [25]. We observed that large ascites were more common in PC patients than PTB patients and had significant differences. As for slight and moderate ascites, there were no significant differences.

Calcified LN which is caused by traces of the TB infection after recovery and the ring enhancement of LN can indicate PTB [26]. Although the amount of these two signs was not large, there was significant difference between two groups. In our study, 38% PTB patients and 26% PC patients had enlarged LN. But there was no significant difference between two groups. The presence of necrotic LN has been considered as a useful indirect sign to rule out PC [27]. However, the two groups had no significant difference on this sign.

The model established in our study showed excellent classification power, whether in the training cohort or the testing

cohort, whereas it was precise enough for clinical use. F1 score provides greater focus on the classification of interest. According to the F1 score, the model also showed good predictive performance in both training and testing cohorts. This implies that the model will show good stability and generalizability in clinical practice.

However, several limitations in this study still exists. First, our study only created a model based on primary CT signs, they were nonquantitative, future study should focus on the quantitative analysis. Second, this study was a retrospective analysis and the number of patients was not very large.

Differentiating PTB from PC has been challenging thus far on CT with many overlapping findings. In conclusion, we created a model based on the clinical characteristics and primary CT signs. The model has significant value in distinguishing PTB from PC. Our study may potentially aid in early differentiation by integrating the multidisciplinary approach currently based on clinical characteristics and primary CT signs. Future large-scale multicenter studies should be carried out to further confirm the results so that this model can be used as a diagnostic tool in routine clinical practice.

Acknowledgements This research was supported by Beijing Key Clinical Specialty Project (20201214) and Leading Talents of Beijing Tongzhou District High Level Talent Development Support Project (YHLD2019029). The funding source provided financial support without any influence on the study design and interpretation of data. We would like to thank our groups from many hospitals for the data collection and interpretation.

Funding Beijing Key Clinical Specialty Project,20201214,Dailun Hou,Leading Talents of Beijing Tongzhou District High Level Talent Development Support Project,YHLD2019029,Dailun Hou

Declarations

Conflict of interest The authors have no conflicts of interest to declare.

References

1. Organization WH, Programme GT. Global tuberculosis report 2021[M]. Available online: <https://www.who.int/teams/global-tuberculosis-programme/tb-reports>.
2. Schito M, Migliori GB, Fletcher HA, et al. 2015 Perspectives on Advances in Tuberculosis Diagnostics, Drugs, and Vaccines. *Clin Infect Dis*. 61Suppl 3(Suppl 3): S102-S118
3. Eraksoy H. Gastrointestinal and Abdominal Tuberculosis. *Gastroenterol Clin North Am*. 2021;50(2):341-360.
4. Sharma MP, Bhatia V. Abdominal tuberculosis. *Indian J Med Res*. 2004;120(4):305-315.
5. Carr NJ. New insights in the pathology of peritoneal surface malignancy. *J Gastrointest Oncol*. 2021;12(Suppl 1):S216-S229.
6. Deshpande SS, Joshi AR, Deshpande SS, Phajlani SA. Computed tomographic features of abdominal tuberculosis: unmask the impersonator! *Abdom Radiol (NY)*. 2019;44(1):11-21.
7. Ramanan RV, Venu V. Differentiation of peritoneal tuberculosis from peritoneal carcinomatosis by the Omental Rim sign. A new sign on contrast enhanced multidetector computed tomography. *Eur J Radiol*. 2019;113:124-134.
8. Yin WJ, Zheng GQ, Chen YF, et al. CT differentiation of malignant peritoneal mesothelioma and tuberculous peritonitis. *Radiol Med*. 2016;121(4):253-260.
9. Husain M, Sachan PK, Khan S, Lama L, Khan RN. Role of diagnostic laparoscopy in chronic and recurrent abdominal pain. *Trop Gastroenterol*. 2013;34(3):170-173.
10. Talat N, Afzal M, Ahmad S, Rasool N, Wasti AR, Saleem M. ROLE OF DIAGNOSTIC LAPAROSCOPY IN EVALUATION AND TREATMENT OF CHRONIC ABDOMINAL PAIN IN CHILDREN. *J Ayub Med Coll Abbottabad*. 2016;28(1):35-38.
11. Sharma V, Bhatia A, Malik S, Singh N, Rana SS. Visceral scalloping on abdominal computed tomography due to abdominal tuberculosis. *Ther Adv Infect Dis*. 2017;4(1):3-9.
12. Choi CH, Kim CJ, Lee YY, et al. Peritoneal tuberculosis: a retrospective review of 20 cases and comparison with primary peritoneal carcinoma. *Int J Gynecol Cancer*. 2010;20(5):798-803.
13. Coccolini F, Gheza F, Lotti M, et al. Peritoneal carcinomatosis. *World J Gastroenterol*. 2013;19(41):6979-6994.
14. Abdelaal A, Alfkey R, Abdelaziem S, et al. Role of laparoscopic peritoneal biopsy in the diagnosis of peritoneal tuberculosis. A seven-year experience. *Chirurgia (Bucur)*. 2014;109(3):330-334.
15. Mazzei MA, Khader L, Cirigliano A, et al. Accuracy of MDCT in the preoperative definition of Peritoneal Cancer Index (PCI) in patients with advanced ovarian cancer who underwent peritonectomy and hyperthermic intraperitoneal chemotherapy (HIPEC). *Abdom Imaging*. 2013;38(6):1422-1430.
16. Charoensak A, Nantavithya P, Apisarnthanarak P. Abdominal CT findings to distinguish between tuberculous peritonitis and peritoneal carcinomatosis. *J Med Assoc Thai*. 2012;95(11):1449-1456.
17. Shim SW, Shin SH, Kwon WJ, Jeong YK, Lee JH. CT Differentiation of Female Peritoneal Tuberculosis and Peritoneal Carcinomatosis From Normal-Sized Ovarian Cancer. *J Comput Assist Tomogr*. 2017;41(1):32-38.
18. Vicens RA, Patnana M, Le O, et al. Multimodality imaging of common and uncommon peritoneal diseases: a review for radiologists. *Abdom Imaging*. 2015;40(2):436-456.
19. Na-ChiangMai W, Pojchamarnwiputh S, Lertprasertsuke N, Chitapanarux T. CT findings of tuberculous peritonitis. *Singapore Med J*. 2008;49(6):488-491.
20. Naz F, Mirza WA, Hashmani N, Sayani R. To identify the features differentiating peritoneal tuberculosis from carcinomatosis on CT scan abdomen taking omental biopsy as a gold standard. *J Pak Med Assoc*. 2018;68(10):1461-1464.
21. Kebapci M, Vardareli E, Adapinar B, Acikalin M. CT findings and serum ca 125 levels in malignant peritoneal mesothelioma: report of 11 new cases and review of the literature. *Eur Radiol*. 2003;13(12):2620-2626.
22. Diop AD, Fontarensky M, Montoriol PF, Da Ines D. CT imaging of peritoneal carcinomatosis and its mimics. *Diagn Interv Imaging*. 2014;95(9):861-872.
23. Akhan O, Pringot J. Imaging of abdominal tuberculosis. *Eur Radiol*. 2002;12(2):312-323.
24. Ladumor H, Al-Mohannadi S, Ameerudeen FS, Ladumor S, Fadl S. TB or not TB: A comprehensive review of imaging manifestations of abdominal tuberculosis and its mimics. *Clin Imaging*. 2021;76:130-143.
25. Souza FF, Jagganathan J, Ramayia N, et al. Recurrent malignant peritoneal mesothelioma: radiological manifestations. *Abdom Imaging*. 2010;35(3):315-321.
26. Pombo F, Díaz Candamio MJ, Rodriguez E, Pombo S. Pancreatic tuberculosis: CT findings. *Abdom Imaging*. 1998;23(4):394-397.

27. Venkata Ramanan R, Pudhiavan A, Venkataramanan A. The "cluster of black pearls" sign of sarcoid lymphadenopathy: a new sign on thin-section contrast-enhanced multidetector CT. *Clin Radiol*. 2017;72(9):729-736.

Publisher's Note Springer Nature remains neutral with regard to jurisdictional claims in published maps and institutional affiliations.

Springer Nature or its licensor (e.g. a society or other partner) holds exclusive rights to this article under a publishing agreement with the author(s) or other rightsholder(s); author self-archiving of the accepted manuscript version of this article is solely governed by the terms of such publishing agreement and applicable law.